



HAL
open science

Derivation of Lanthanide Series Crystal Field Parameters From First Principles

Julie Jung, Md. Ashraful Islam, Vincent Pecoraro, Talal Mallah, Claude
Berthon, H el ene Bolvin

► **To cite this version:**

Julie Jung, Md. Ashraful Islam, Vincent Pecoraro, Talal Mallah, Claude Berthon, et al.. Derivation of Lanthanide Series Crystal Field Parameters From First Principles. Chemistry - A European Journal, 2019, 25 (66), pp.15112-15122. 10.1002/chem.201903141 . hal-02381772

HAL Id: hal-02381772

<https://hal.science/hal-02381772>

Submitted on 18 Feb 2020

HAL is a multi-disciplinary open access archive for the deposit and dissemination of scientific research documents, whether they are published or not. The documents may come from teaching and research institutions in France or abroad, or from public or private research centers.

L'archive ouverte pluridisciplinaire **HAL**, est destin ee au d ep ot et  a la diffusion de documents scientifiques de niveau recherche, publi es ou non,  emanant des  tablissements d'enseignement et de recherche fran ais ou  trangers, des laboratoires publics ou priv es.

Derivation of Lanthanide Series Crystal Field Parameters From First Principles.

Julie Jung^a, Md. Ashraful Islam^b, Vincent L. Pecoraro^c, Talal Mallah^d, Claude Berthon^e,
Hélène Bolvin^{b f *}

Abstract

Two series of lanthanide complexes have been chosen to analyze trends in the magnetic properties and crystal field parameters (CFPs) along the series: the highly symmetric $\text{LnZn}_{16}(\text{picHA})_{16}$ series with $\text{Ln} = \text{Tb}, \text{Dy}, \text{Ho}, \text{Er}, \text{Yb}$ and $\text{picHA} = \text{picoline hydroxamic}$, and the $[\text{Ln}(\text{DPA})_3](\text{C}_3\text{H}_5\text{N}_2)_3 \cdot 3\text{H}_2\text{O}$ series with $\text{DPA} = 2,6\text{-dipicolinic acid}$ and $\text{Ln} = \text{Ce-Yb}$ and with approximate three-fold symmetry. The first series presents a compressed coordination sphere of 8 oxygen atoms environment while in the 2nd series, the coordination sphere is formed by an elongated coordination sphere formed by six oxygen atoms. CFPs are deduced from *ab initio* calculations using two methods: the AILFT (Ab Initio Ligand Field Theory) which determines the parameters at the orbital level, and the ITO (Irreducible Technique Operator) decomposition which treats the problem at the many-electron level. It is shown that the CFPs are transferable from one derivative to the other, within a given series, as a first approximation. The sign of the 2nd order parameter B_0^2 differs in the two series reflecting the different environments. It is shown that the use of strength parameter S allows for an easy comparison between complexes. Furthermore, in both series, the parameters are found to decrease in magnitude along the series and this decrease is imputed to covalent effects.

Introduction

With the discovery of lanthanides as Single Ion Magnets [1], there has been a resurgence of synthetic activity for new lanthanide complexes. Crystal field (CF) theory has been widely used to rationalize the properties of those complexes, in particular the nature of the ground state, and the anisotropy of the magnetic properties. Crystal field parameters (CFPs) play a key role in the modelization of pNMR shifts in lanthanide complexes, according to the theory proposed by Bleaney in the 70's. CF theory models the splitting of the metal orbitals, either d or f , in the presence of the ligands [2]. First proposed for the d elements for transition metal complexes as a pure electrostatic interaction [3, 4], Racah and Stevens applied the Wigner-Eckart theorem to simplify the evaluation of the CF matrix elements for many-electron cases [5, 6]. Since then, the formalism has been extended to the f elements [7]. It provides a theoretical framework for modelling the ion environment by means of few parameters. CFPs are considered as phenomenological parameters, and are fitted against experimental data.

For lanthanide containing complexes, the interaction between the lanthanide ion and the ligands has always been considered to be mostly electrostatic in nature. The nature of the ground state has been, therefore, rationalized using electrostatic arguments; two softwares, CONDON and PHI, were developed for an efficient fitting of the CFPs against experimental data [8, 9]. On an electrostatic basis and for highly symmetrical molecules, Rinehart and Long have shown that the shape of the ligand environment allows to predict the nature of the low-lying M_J states and thus the magnetic behavior of the complexes [10]. This model holds in a high symmetry environment. To describe less symmetrical environments, computational approaches have been recently proposed: i) by combining an electrostatic description with semi-empirical radial effective charges (REC) [11], ii) by describing the ligands by charges either optimized to fit the experimental data within the lone pair effective charge (LPEC) model [12] or taken from *ab initio* calculations (CAMEL) [13]. A purely electrostatic approach has been proposed in order to determine the

^aTheoretical division, Los Alamos National Laboratory, Los Alamos, New Mexico 87545, USA.

^bLaboratoire de Chimie et Physique Quantiques, CNRS, Université Toulouse III, 118 route de Narbonne, 31062 Toulouse, France.

^cDepartment of Chemistry, Willard H. Dow Laboratories, University of Michigan, Ann Arbor, Michigan, 48109, USA.

^dInstitut de Chimie Moléculaire et des Matériaux d'Orsay, CNRS, Université de Paris-Sud 11, 91405 Orsay Cedex, France.

^eCEA, Nuclear Energy Division, Radiochemistry Processes Department, DRCP, BP 17171, F-30207 Bagnols sur Cèze, France.

^fLaboratoire de Chimie et Physique Quantiques, CNRS, Université Toulouse III, 118 route de Narbonne, 31062 Toulouse, France.

*e-mail address: bolvin@irsamc.ups-tlse.fr

direction of the magnetic moment, by minimizing the potential energy; the ligands are modeled by fractional charges determined by valence bond resonance hybrids [14].

Even through the lanthanide ion–ligand interaction is predominately electrostatic, some degree of covalency has been evidenced, but to a lesser extent than for the $5f$ elements. The $5d$ and $6s$ orbitals participate the most in the mixing, due to the inner-shell character of the $4f$ orbitals [15, 16, 17]. First principles calculations allow for an accurate description of bonding, describing correctly both electrostatic and the tiny covalent bonding effects. They have become a useful tool to interpret magnetic data of lanthanide complexes, by providing the nature of the ground state and the associated magnetic moment as well as the nature of the low lying states that may be involved in relaxation processes [18], and are a useful support for the interpretation of experimental data in lanthanide complexes [19]. More recently, *ab initio* calculations have also been successful in describing the magnetic coupling between two lanthanide centers [20]. Magnetic anisotropy is modeled by the so called g tensor and the splitting of the ground manifold by the ligands in absence of magnetic field by the zero-field splitting (ZFS) tensor. These model parameters can be obtained from fitting experimental data with a model Hamiltonian, and from *ab initio* calculations [21, 22]. In transition metal complexes, the ZFS is induced by the spin-orbit coupling with excited states [23], while in f elements it arises from the splitting of the ground J multiplet of the free ion by the ligands, and is characterized by the CFPs. In principle, the ZFS needs 27 independent parameters, which number is reduced by symmetry. For example, in octahedral symmetry, only two CFPs are left, and they are easily deduced from both experimental data and calculation by fitting the energies of the states [24]. For lower symmetry, the number of CFPs increases, and at some point, it is no longer possible to evaluate those parameters neither from experimental data nor from computed energies of the levels. However, all information is available from *ab initio* calculations and two methods have recently been proposed for this purpose.

The aim of this work is to analyze the correlations between the structure and the CFPs deduced from *ab initio* calculations, and to the expected magnetic properties according to their prolate or oblate shape in two series of lanthanide complexes. The advantage of using *ab initio* calculations is threefold; i) all types of interactions are taken into account, not only the electrostatic ones, ii) the 27 CFPs can be determined in the case of low symmetry, iii) the relevance of CF theory to model the low lying spectrum can be assessed. In the first series, denoted LnZn_{16} , the lanthanide ion is sandwiched by metal-lacrown species to form a quasi-perfect compressed

\mathcal{D}_{4d} symmetry, which reduces the number of CFPs [25, 26, 27]. This is a rare case where the qualitative electrostatic model of Rinehart and Long applies almost perfectly. The second series, denoted $[\text{Ln}(\text{DPA})_3]^{3-}$, covers the whole period, the environment is more prolate, and it is close to a three fold symmetry, but not strictly [28]. As will appear from the calculations, the magnetization stays axial along the series with a variation in the direction. Furthermore, the 2nd order parameter was recently deduced from paramagnetic NMR, applying Bleaney’s theory [28].

CFPs were deduced from *ab initio* calculations, comparing different methods. They are determined from the energy matrix written either in the basis sets of the orbitals (*Ab Initio* Ligand Field Theory, AILFT) [29], or in the basis set of the many-electron wave functions (Irreducible Technique Operator, ITO) [30]. Since the first series is highly symmetrical, CFPs could be directly fitted on the energies. This work completes a previous publication where an other question about CFPs was addressed, namely the transferability of the CFPs from the orbital picture to the many-electron picture including spin-orbit coupling. It came out of this study that covalent effects between the metal and the ligands affect the CFPs, even for the ionic PrCl_3 crystal [31]. This will be confirmed by the present work where we aim at addressing the following points i) Do the two above-mentioned methods provide similar CFPs? ii) Are the CFPs transferable within each series as they depend only on the nature and the position of the ligands? iii) How to connect the CFPs to magnetic properties? iv) Are the trends across the series impacted by covalent effects?

While the two series are described in the first Section, the main features of the methods for the determination of the CFPs from *ab initio* calculation are exposed in the second Section, with more details provided in the SI (Sections S1 and S2). Finally, in third Section, the CFPs are calculated for the two series mentioned above and the trend in the computed CFPs are discussed.

Two lanthanide series

LnZn_{16}

The isostructural $\text{LnZn}_{16}(\text{picHA})_{16}$ series with $\text{Ln} = \text{Tb}, \text{Dy}, \text{Ho}, \text{Er}$ and $\text{picHA} = \text{picoline hydroxamic acid}$ has been synthesized by Pecoraro *et al.*, and characterized by magnetometry [25, 27]. It has been completed by $\text{YbZn}_{16}(\text{pyzHA})_{16}$ with $\text{pyzHA} = \text{pyrazine hydroxamic acid}$, which is isostructural with the previous series, and possesses attractive near-infrared (NIR) emission properties [26]. The

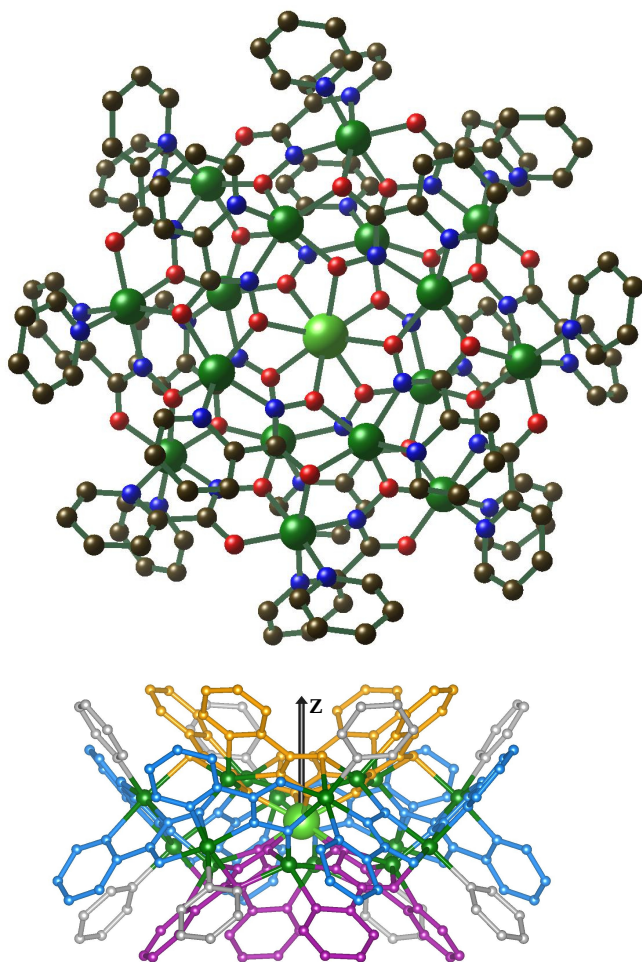


Figure 1: Structure of LnZn_{16} complexes [25]. Top: top view green: Er, Zn, red: O, blue: N, black: C. Bottom side view: purple: upper 12-MC-4, orange: lower 12-MC-4, blue: 24-MC-8 ring, grey: pyridine. Hydrogens have been omitted for clarity.

structure of the lighter lanthanides, when available are structurally different due to the presence of water molecules in the coordination sphere. In this series, two 12-MC-4 (MC = metallacrown) sandwich a Ln(III) ion, and a further 24-MC-8 ring lies around this sandwich through π -stacking interactions between the picHA rings (see Figure 1). The Ln(III) ions are surrounded by eight oxygen atoms forming a compressed square antiprism geometry very close to a perfect D_{4d} symmetry. The Ln-O distance ranges from 2.35 (Tb) to 2.31 Å (Yb) following the diminution of the ionic radius in the series. The angle with the quaternary axis is constant and about 62.3° which denotes a compressed environment. As described in [26, 27], this compressed environment leads to unusual magnetic properties, with axial and planar magnetizations for Er(III) and Dy(III) complexes, respectively.

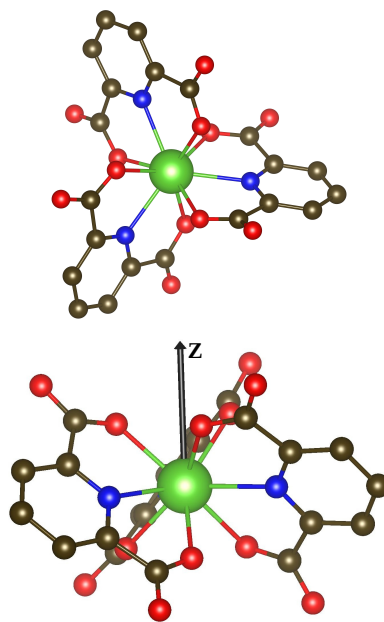


Figure 2: $[\text{Ln}(\text{DPA})_3]^{3-}$ complex. Top: top view, Bottom: side view green: Ln, red: O, blue: N, black: C. Hydrogens have been omitted for clarity.

$[\text{Ln}(\text{DPA})_3]^{3-}$

The $[\text{Ln}(\text{DPA})_3](\text{C}_3\text{H}_5\text{N}_2)_3 \cdot 3\text{H}_2\text{O}$ series (denoted $[\text{Ln}(\text{DPA})_3]^{3-}$) is isostructural. The complexes have been structurally characterized by X-ray diffraction for Ln = Ce - Yb except Pr and crystallizes in a triclinic space group $P1$ [28]. The coordination sphere contains three DPA^- forming a tricapped trigonal distorted prism (see Figure 2). Each ligand is tridentate, and coordinated to the Ln(III) cation through the nitrogen atom of the pyridine cycle (capped position), and the two oxygen atoms of the carboxylate groups (prism position). The coordination sphere is formed by 6 oxygen and 3 nitrogen atoms with distances ranging from 2.51 (Ce-O) to 2.37 Å (Yb-O), and 2.63 (Ce-N) to 2.45 Å (Yb-N). Due to the presence of counterions, the ternary symmetry is slightly distorted and for a given complex, the distances between the metal ion and the three ligands differ by about 0.1 Å. The oxygen atoms are closer than the nitrogen ones, and are more electronegative, as confirmed by the Mulliken charges of circa -0.9 and -0.2 respectively. One might expect the oxygen atoms to dominate the crystal field. The angle between the oxygen atoms with the pseudo ternary axis is rather constant along the series around 46° ; this is a much smaller value than in the LnZn_{16} series and denotes a prolate environment.

The whole $[\text{Ln}(\text{DPA})_3]^{3-}$ series is considered in this work, except the Gd complex, which has a pure spin ground state, and where the ZFS arises from second order interactions. The Z axis is perpendicular to the plane formed by the three nitrogen atoms, while X and Y axes are arbitrary (see Figure 2).

Crystal field parameters

Model Hamiltonian within crystal field theory

The Hamiltonian describing the f electrons may be written as

$$\hat{\mathcal{H}}^{CF} = \sum_{i=1}^N \left[\hat{T}_i - \frac{Z^*}{r_i} \right] + \sum_{i<j} \frac{1}{r_{ij}} + \sum_{i=1}^N \left(\xi \hat{\mathbf{l}}_i \cdot \hat{\mathbf{s}}_i + \hat{v}^{CF}(\mathbf{r}_i) \right) \quad (1)$$

with the scalar relativistic kinetic term, the attraction of the electrons by the screened charge of the metal nucleus Z^* , the electron-electron repulsion, the spin-orbit operator, and the one-electron CF operator, respectively. The sum runs over the N f electrons of the valence shell. The many-electron CF operator is the sum of the one-electron operators

$$\hat{V}^{CF} = \sum_{i=1}^N \hat{v}^{CF}(\mathbf{r}_i) \quad (2)$$

where \hat{v}^{CF} is the electrostatic potential at a point \mathbf{r} close to the magnetic center arising from the ligands represented by point charges. In its pure electrostatic formulation, it arises from the charges attributed to the ligands and it is written as a multipolar expansion in terms of spherical coordinates

$$\hat{v}^{CF}(\mathbf{r}) = \sum_{k=0}^{\infty} \sum_{q=-k}^k b_k^q r^k Y_k^q(\theta, \phi) = \sum_{k,q} \hat{v}_k^q(\mathbf{r}) \quad (3)$$

The $\hat{v}_k^q(\mathbf{r})$ are components of irreducible tensors of rank k , and their matrix elements within a f^N configuration with pure f orbitals vanish for $k > 6$ as well as for odd values of k . The first term, with $k = 0$, does not contribute to CF splitting [32]. The non-contributing terms (k, q) are usually omitted in the expansion of Eq. 3 and the number of terms is further reduced by symmetry.

Assuming that all the $4f$ orbitals have the same spatial expansion, the \hat{v}_k^q operators (or their many-electron counterpart) acting in the Hilbert space of the Slater determinants may be replaced by the tensor operators \hat{O}_k^q acting in either the l (one-electron), L (spin-free) or J (spin-orbit) manifolds. Eq. 2 is then equivalent to

$$\hat{V}^{CF}(X) = \sum_{k=2,4,6} \alpha_X^k \sum_{q=-k}^k B_q^k \hat{O}_q^k(X) \quad (4)$$

where $X = l, L, J$ according to the considered manifold. The $\alpha_X^k = \langle X || \alpha^k || X \rangle$ are the reduced matrix elements of 2nd, 4th and 6th order respectively. The α_l^k are determined by N , the α_L^k by N and L ,

and the α_J^k by N, L and J . These reduced matrix elements are tabulated for the ground state of each lanthanide ion [32]. The convention of Wybourne is used throughout this work [7, 33]. It has been very early understood that the pure electrostatic picture is by far not quantitative. Since the incorporation of some covalency keeps the one-electron structure, \hat{V}_{CF} may be seen as an effective interaction which parameters are fitted on experimental data. We showed in a recent article [31] that the CFPs deduced from orbital energies ($X = l$), and from many-electron wavefunctions without or with spin-orbit coupling ($X = L$ and J respectively) lead to similar CFPs. Consequently, the reduced elements α_X^k depend on the nature of the metal, and the CFPs B_q^k only on the nature and position of the ligands, and should be transferable within the lanthanide series.

The CFPs depend on the orientation of the molecule in the $\{X, Y, Z\}$ frame. They are in general imaginary, and rotations about Z axis affect the phase factor mixing B_q^k and B_{-q}^k . In the present work, Z is chosen as the pseudo rotation axis (cf Fig. 1 and 2), and the choice of X and Y axes is arbitrary. Hence, only the norm of these parameters is considered in this article [34]

$$\bar{B}_q^k = \sqrt{|B_q^k|^2 + |B_{-q}^k|^2} \quad (5)$$

For the sake of comparison, rotational invariant are considered in order to reduce the numerous CFPs to fewer parameters, more specifically the second order moments [35, 36]. We considered the strength parameter of k th order

$$S^k = \left[\frac{1}{2k+1} \sum_{q=-k}^k |B_q^k|^2 \right]^{1/2} \quad (6)$$

and the strength parameter as defined by Chang [35]

$$S = \left[\frac{1}{3} \sum_k \frac{1}{2k+1} \sum_{q=-k}^k |B_q^k|^2 \right]^{1/2} \quad (7)$$

These two strength parameters are rotational invariant. In order to quantify the symmetry about the Z axis, the strength parameter of q th index was considered

$$S_q = \left[\sum_k \frac{1}{2k+1} |B_q^k|^2 \right]^{1/2} \quad (8)$$

This parameter is not a rotational invariant but it is invariant according to rotations about Z axis. Eqs. 6, 7 and 8 are related by

$$\begin{aligned} S &= \sqrt{\frac{S^2 + S^4 + S^6}{3}} \\ &= \sqrt{\frac{S_0 + S_1 + S_2 + S_3 + S_4 + S_5 + S_6}{3}} \end{aligned} \quad (9)$$

The parameter S allows to evaluate the strength of the ligand field with only one parameter and gives an idea of the overall splitting of the ground J manifold.

Crystal field parameters from first principles

The CFPs model the splitting of a J multiplet of the free ion by the ligands, and according to CF theory, there are 27 such parameters. The CF operator of Eq. 3 is essentially a one-electron operator which acts at the orbital level. By applying the Wigner-Eckart theorem, it may be expressed as a many-electron operator acting in a given J manifold (Eq. 4) [5, 6]. In transition metal complexes, the ZFS arises due to spin-orbit coupling with excited states and the analysis at the orbital level needs symmetry considerations [37]; in lanthanide complexes, CFPs determined at the orbital or many-electron levels are similar because the splitting of the $4f$ orbitals by the CF is sufficiently small not to impact the composition of the many-electron wave functions of the free ion [31]. Once the CFPs are known, the energy and composition of the $2J + 1$ states arising from this manifold are fully characterized, and all magnetic and spectroscopic properties may be deduced.

Ab initio calculations based on CASSCF method provide the energy of the low lying states, and their composition in terms of Slater determinants, which provides the necessary information for the determination of the CFPs. The AILFT method developed by Atanasov considers the CF operator in its one-electron picture, and additional parameters are needed to model the two-electron interaction (Slater-Condon parameters), and the spin-orbit interaction [29]. On the other hand, the ITO method proposed by Chibotaru and Ungur considers the CF operator in its operator equivalent picture, and the CFPs are deduced from the many-electron energies and wavefunctions of the considered J manifold [30]. The determination of spin Hamiltonian parameters from *ab initio* calculations needs the one-to-one correspondence between the computed and model states, and this is usually a key stage of the procedure [38, 39, 22]. For AILFT, the correspondence is performed at the one-electron level by mapping the seven $4f$ orbitals, while for ITO, it is performed by determining the eigenvectors of the magnetic moment operators. Finally, AILFT deduces the CFPs from a fitting procedure while ITO method performs a decomposition using irreducible tensor operators technique.

Fitting procedure (FIT)

In the case of complexes with high symmetry, the number of CFPs is reduced. In octahedral symmetry, there are two independent parameters [40], and the CFPs are easily deduced from *ab initio* calculations [24]. When an axial symmetry is present, there are only three CFPs left: B_0^2 , B_0^4 and B_0^6 . In this case, the parameters can be fitted against the *ab initio* energies by a least square procedure when J is large enough. Then, the states are assigned according to the projection of the total angular momentum \hat{J}_Z . This method is applied to the LnZn₁₆ series which evidences a symmetry very close to \mathcal{D}_{4d} . This is still feasible when few off diagonal terms are present ($q \neq 0$) like for \mathcal{D}_{3h} with an additional B_6^6 term [31].

Ab initio ligand field theory (AILFT)

The second approach has been developed by Atanasov, first based on DFT calculations [41], and afterwards adapted to WFT [42]. It has been applied to octahedral series of lanthanide [43] and actinide [44]. The many-electron wave-functions of a $4f^N$ ion are written as linear combinations of Slater determinants $|\phi_i \cdots \phi_j|$ built with real $4f$ spin-orbitals ϕ_i . Since $4f$ orbitals are very inner shell, the ϕ_i are almost of pure $4f$ character. The correspondence with the model space is performed at this stage. Both the *ab initio* and the model Hamiltonians of Eq. 1 are expanded in the Slater determinants basis, and there is a one-to-one correspondence of the matrix elements. The model matrix is expressed with the 27 CF matrix elements, the three Slater-Condon parameters for electron-electron repulsion F^2 , F^4 and F^6 [45], and the effective one-electron spin-orbit coupling parameter ζ . These parameters are deduced by equating the matrix elements of the *ab initio* and model matrices. The system of equations is overparametrized, and is solved through a least square procedure. More details are given in Section S1.

Irreducible Tensor Operator (ITO) method

This method has been proposed by Ungur and Chibotaru [30]. The CFPs are deduced from the $2J + 1$ wave-functions, and corresponding energies of a J term of the free ion. This assumes that this manifold is well separated from the other ones, and easily identifiable. Since the *ab initio* eigenvectors of the Z component of the total angular magnetic moment \hat{M}_Z correspond to the model $\{|J, M_J\rangle\}$ vectors, the one-to-one correspondence is performed by diagonalizing the representation matrix of \hat{M}_Z in the J manifold. The phase factors between the states is further determined such that the superdiagonal of the representation matrix of \hat{M}_X is real. The *ab*

initio Hamiltonian matrix is then expressed in this new basis set, and is decomposed in terms of spin matrices of the ITOs [46, 47]. The corresponding projections are the CFPs within the reduced matrix elements α_j^k of Eq. 4. Since CFPs are obtained by a decomposition technique, there is no loss of information but the $2J + 1$ degrees of freedom reduce naturally to the 27 ones: while the odd order parameters vanish because of time-reversal symmetry of the Hamiltonian, parameters with $k > 6$ appear to be negligible. The similarity between the *ab initio* \mathbf{M}_u^J and the model \mathbf{M}_u^{AI} matrices in direction u is quantified by the distance between those matrices as

$$\delta m_u = \sqrt{\text{Tr} \left(\mathbf{M}_u^J - \mathbf{M}_u^{AI} \right)^\dagger \left(\mathbf{M}_u^J - \mathbf{M}_u^{AI} \right)} \quad (10)$$

where \dagger denotes the conjugate transpose. δm_u vanishes in the limit of the free ion in the LS coupling scheme. An another index, δh , is introduced for quantifying the similarity between the *ab initio* and model Hamiltonian representation matrices (see Eq. S8). More details are given in Section S2.

Results and discussion

LnZn₁₆

The axial symmetry leads to a reduced number of CFPs, namely B_0^2 , B_0^4 and B_0^6 , which can be fitted either against experimental data or *ab initio* results. In this work, we compare CFPs determined from *ab initio* calculations with both FIT and ITO methods. CFPs obtained for the five complexes are summarized in Table S1, and represented in Figure 3. The energies of the ground J manifold are given in Table S2. The two methods lead to identical values. With ITO, due to a small twist angle around the Z axis slightly breaking the \mathcal{D}_{4d} symmetry, some CFPs with $q \neq 0$ are non zero, as for example B_4^4 and B_4^6 .

B_0^2 is the largest in magnitude, and negative as expected from a compressed environment. This negative value of B_0^2 leads the magnetization to be axial in the Er derivative, and planar in the Dy derivative [10, 31]. B_0^4 and B_0^6 are by far non negligible around $\pm 500 \text{ cm}^{-1}$, and opposite in sign, which leads to entangled spectra in terms of $|M_J|$. As discussed in reference [31], α_j^2 changes sign between Ho and Er. This impacts the ordering of the states in terms of $|M_J|$: for Tb and Dy, $|M_J|$ increases with the energy, for Yb, it decreases. For Ho and Er complexes, states are more entangled due to the important values of B_0^4 and B_0^6 which lead to non quadratic relation between the energy and $|M_J|$. All CFPs decrease in magnitude along the series which will be further discussed in the last Section

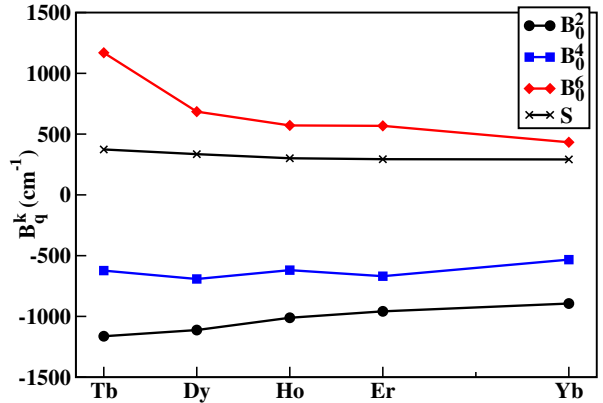


Figure 3: CFPs and strength parameter (cm^{-1}) in the LnZn₁₆ series using ITO method. For HoZn₁₆, averaged over DyZn₁₆ and ErZn₁₆ structures.

and consequently, the strength parameter S defined in Eq. 7 follows this trend.

[Ln(DPA)₃]³⁻

Since the real and imaginary parts of the non diagonal CFPs vary by any rotation in the XY plane, only their norm is considered, \overline{B}_q^k as defined in Eq. 5. CFPs were calculated with both AILFT and ITO. For ITO, the manifolds with $J < 3$ do not provide CFPs of 6th order since the expansion of Eq. S5 is limited to $2J$. This artificially leads to smaller strength parameters S and S_q due to the restricted sum of terms (see Eqs. 7 and 8). To overcome this limitation, the CFPs of 6th order (and all orders for Eu(III)) are deduced from the 1st excited J manifolds.

All CFPs are given in Tables S6 and S7, and strength parameters in Tables S8 and S9. The dominant parameters are represented in Figures 4 and 5, while the others are shown in Figures S2. The two methods give similar CFPs. This confirms that CFPs extracted from orbital and many-electron levels are very close due to the small ZFS of the $4f$ orbitals. It should be outlined that the energy of the low lying excited states are very similar, even through calculated with different codes, different basis sets, and slightly different approximations (see Table S3). While B_0^2 , B_0^4 , B_0^6 , B_3^4 , B_3^6 , and B_6^6 are worth several hundred wavenumbers, all the other parameters are smaller than 100 cm^{-1} . This is in agreement with the approximate threefold symmetry of the complexes. Indeed, within the trigonal C_3 point group, only those six CFPs would be non zero. B_0^2 is positive while B_0^4 and B_0^6 are negative, and the three CFPs are of the same order of magnitude. The sign of B_0^2 is opposite to that of the LnZn₁₆ series, which denotes a more prolate coordination environment. As in the other studied complexes, the CFPs are transferable along the series with an overall decrease in magnitude. This confirms that the

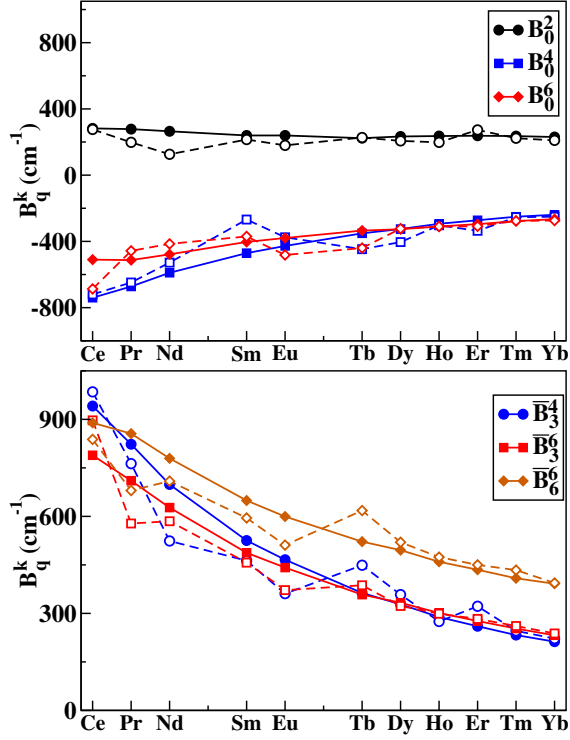


Figure 4: CFPs (cm^{-1}) in the $[\text{Ln}(\text{DPA})_3]^{3-}$ series. full line: AILFT; dashed line: ITO.

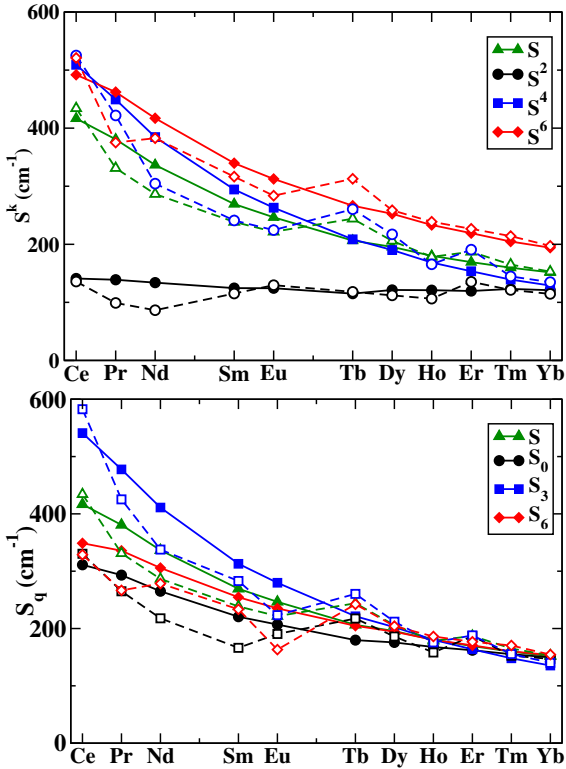


Figure 5: Strength parameters (cm^{-1}) in the $[\text{Ln}(\text{DPA})_3]^{3-}$ series. full line: AILFT; dashed line: ITO.

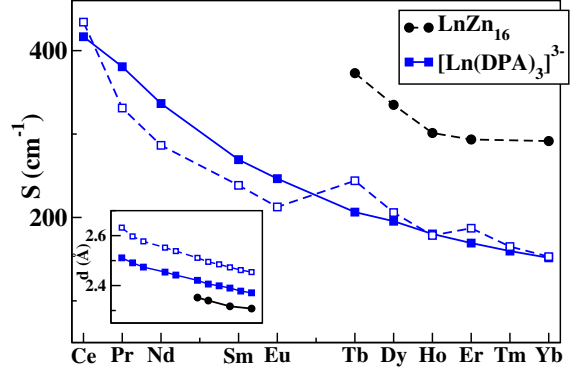


Figure 6: Strength parameter (cm^{-1}) in the LnZn_{16} and $[\text{Ln}(\text{DPA})_3]^{3-}$ series. Full line: AILFT, dashed line: ITO. Inset: averaged bond distance in the coordination sphere: LnZn_{16} 8 oxygen atoms, $[\text{Ln}(\text{DPA})_3]^{3-}$ full line 6 oxygen atoms, dashed line 3 nitrogen atoms.

effects of ligands and central ion are decoupled and independently described by the parameters B_q^k and α_J^k of Eq. 4 respectively.

In the case of axial symmetry complexes, the nature of the ground state magnetization alternates between planar and axial following the sign of α_J^2 from Eq. 4. In the LnZn_{16} series, B_0^2 is negative, and the magnetization is planar for the Dy derivative, and axial for the Er one. For sandwich complexes [31], B_0^2 is positive for benzene and cyclopentadienyl ligands and negative for the more compressed COT environment leading to opposite magnetic anisotropies for those different ligands. In the $[\text{Ln}(\text{DPA})_3]^{3-}$ series, B_0^2 is positive as expected from the prolate layout of the oxygen atoms. Hence, one would expect a planar (axial) magnetization for Sm, Er and Yb (Ce, Nd and Dy) due to a positive (negative) value of α_J^2 . However, this is not the case as can be seen from the g factors of the ground Kramers doublets given in Table S5. Since the 4th and 6th orders CFPs, as well as the ternary non-diagonal parameters are non negligible, the ground states are by far not pure M_J eigenstates. The Dy complex shows an axial magnetization, and so do the Er and Yb ones with a magnetization in a direction perpendicular to the ternary axis. This is in agreement with previous observations [48, 49]: in the presence of pseudo-axial symmetry, the magnetic anisotropy of elongated Er derivatives, which is expected to be planar, is axial and oriented perpendicularly to the pseudo axis. As a consequence, magnetic axes of the Dy and Er complexes are perpendicular.

Trends in the Ln series

Strength parameters and CFPs

The strength parameters are represented for the two series in Figure 6 and compared to metal-ligand dis-

tances. As discussed in Section 3, the strength parameter S defined by Eq. 7 gathers in only one parameter the 27 CFPs and allows an easy evaluation of the strength of the metal-ligand interaction. This facilitates the comparison between two complexes. Along the two series, the coordination sphere shrinks following the reduction of the ionic radius of the free ion. The CFPs decrease in magnitude along the two series. S is larger in the LnZn_{16} than in the $[\text{Ln}(\text{DPA})_3]^{3-}$ series. In a pure electrostatic picture, according to Eq. 3, the CFPs are determined by the position and the charge of the ligands, as well as by the radial expansion of the $4f$ orbitals. Along the series, the nuclear charge of the lanthanide atom increases, the $4f$ orbitals become more inner shell, the ionic radius of the free ion decreases and, accordingly, the coordination sphere shrinks. In an isostructural series, the structural changes are smooth and, as a first approximation, since they are determined only by the ligands, the CFPs may be considered as transferable from one lanthanide ion to another one inside a series as observed by Bleaney [32]. The variation of the number of $4f$ electrons is included in the α_X^k reduced matrix elements, and the variation of the α_X^k , both in amplitude and in sign, leads to very different energetic spectra and magnetic behavior from one lanthanide ion to the other one.

Figure 6 denotes a smooth variation of the CFPs; one may say, as a first approximation, that they are transferable from one ion to the next one with a small variation. But one may not say that they are constant in the whole series. As was shown in reference [31], the trends in the many-electron spectra are much more tricky to analyze, because of the large variation of the α_X^k , especially of α_X^2 which changes three times of sign along the series. In the LnZn_{16} series, except for B_0^6 in the $\text{Tb}(\text{III})$ complex, the three CFPs are rather constant, as they only decrease by 10 - 20 % in magnitude (see Figure 3). δm_u defined in Eq. 10 with $u = X, Y, Z$ (see Table S1), which quantifies the similitude of the \hat{M}_u matrix to that of the free ion in the LS coupling scheme, decreases in the series to be almost 0 for Yb. The same tendency is observed for δh (defined in Eq. S8), which quantifies the similitude between the *ab initio* and the model matrices expanded up to the 6th order.

Point charge model

In order to analyze those variations, a point charge (PC) model has been considered, where each atom of the ligands is represented by a PC deduced from its LoProp *ab initio* value [50]. The electrostatic potential created by the PC model and the *ab initio* ligands are similar (see Table S10). The PC and *ab initio* strength parameters are compared in Figure 7. The PC strength parameter is rather con-

stant in the series. Since the dipole and quadrupole moments determined from both models are almost identical, the difference between PC and *ab initio* calculations represent covalent contributions, which include combined effects of bonding, charge donation and polarization. In the electrostatic model, the CF is axial and dominated by 2nd order terms (S^2 and S_0 dominant), while the other terms are almost negligible. This prevalence of the 2nd order for electrostatic models was already observed in PrCl_3 and sandwich complexes [31]. It confirms that 4th, 6th and non axial contributions arise mostly from non electrostatic effects, as polarization of f orbitals, orthogonality issues, electron correlation and covalent effects. As already mentioned, the PC model leads to a rather constant value of S . The difference between the *ab initio* and the PC curves is rather constant for the 2nd order, and tends to decrease for the 4th and 6th orders. It should be mentioned that a simplified PC model, where ligands are replaced by only nine point charges placed at the position of the six oxygen and three nitrogen atoms of the coordination sphere leads to similar results as the more sophisticated PC model (see Fig. S6).

In a pure electrostatic picture, the closer the charges, and hence, the larger the interaction and the CFPs. In the LnZn_{16} series, the coordination sphere is more compressed than in the $[\text{Ln}(\text{DPA})_3]^{3-}$ series and S is larger since the ligands are closer to the $4f$ electrons. But the trend along a series is not as simple since there are two opposite effects: i) according to the contraction of the $4f$ orbitals, the CFPs should decrease but ii) following the shrinking of the coordination sphere, the CFPs should increase. In order to unravel those two effects, they were dissociated by varying independently the nature of the Ln ion and the position of the charges (see Section S4.5). As expected, the CFPs decrease when changing the metal ion (fixed position of the point charges), and increase when changing the position of the charges (fixed Ln). The contraction of the coordination sphere and the decrease in the spatial distribution of the $4f$ electrons lead to opposite trends along the series, and the interweaved effects lead to a rather constant value of S . Consequently, the decrease of the strength parameters which is observed in Figure 6 with the full ligands arises from the overlap between the lanthanide and ligand orbitals, namely covalent effects. The $4f$ being inner shell, they participate little to the covalent bonding itself, which involves mostly $5s$, $5p$ and $6d$ orbitals. It was shown in reference [31], that both the direct overlap between the $4f$ and the orbitals of the ligands, and the indirect interaction through the more outer shell orbitals affect the CFPs. As in this previous work, covalent effects reduce the CFPs of 2nd order and increase the other CFPs, and more specifically the off diag-

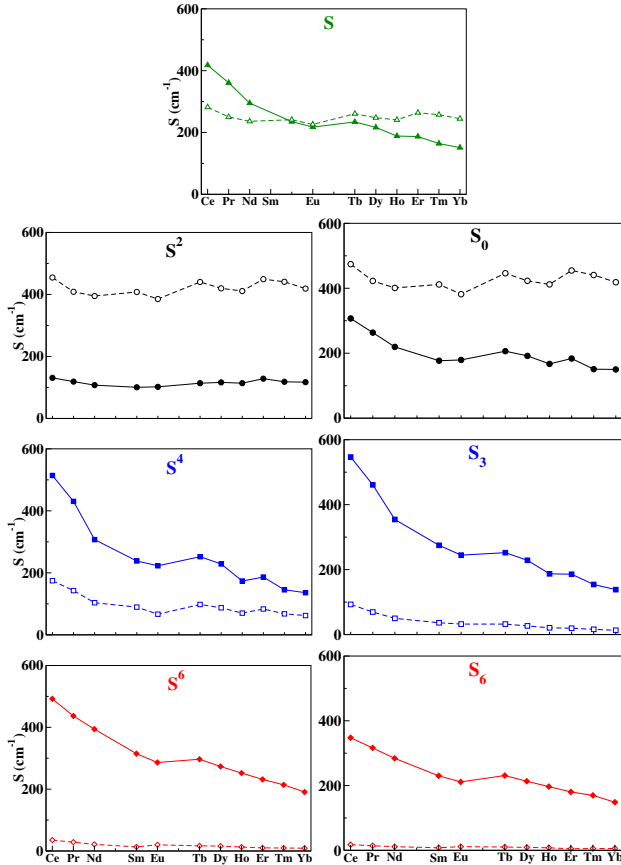


Figure 7: Strength parameters (cm^{-1}) in the $[\text{Ln}(\text{DPA})_3]^{3-}$ determined by ITO method; full line *ab initio*, dashed line, PC model.

onal terms with $q \neq 0$.

The decrease of the CFPs in the lanthanide series has been observed previously. Duan *et al.* fitted the energetic spectra of the whole series of $\text{Cs}_2\text{NaLnCl}_6$ [51] taking advantage of the octahedral symmetry, which leads to only two non vanishing independent CFPs. Both B_0^4 and B_0^6 decrease in the series, respectively, from 2100 ($\text{Ln}=\text{Ce}$) to 1400 ($\text{Ln}=\text{Yb}$) and from 260 to 90 cm^{-1} . The authors showed that this decrease is larger than the one expected by a pure PC model for the ligands. Faulkner *et al.* [52] improved the PC model by adding induced dipoles on the ligands, and this lead to a decrease in the CFPs. But the present work shows that the extended PC model leads to similar results than the one with only nine PCs. Ishikawa *et al.* deduced the CFPs in the $[\text{Pc}_2\text{Ln}]^-$ series for the second part of the Ln series by fitting paramagnetic shifts and magnetic susceptibilities [53]. Both B_0^2 and B_0^4 decrease in magnitude while B_0^6 is rather constant, but small.

Comparison ITO/AILFT

In the $[\text{Ln}(\text{DPA})_3]^{3-}$ series, the variation of the CFPs along the series is smoother with AILFT than with ITO (see Figure 4). In the first half,

the ITO values are smaller than the AILFT values, while the opposite trend is found in the second half. Also, there are more irregularities in the ITO values, especially in the first half of the series. In the first half, the value of J is small according to the 3rd Hund's rule, and the different J manifolds are closer to each other according to Landé rule. One could suspect the spin-orbit coupling between the J manifolds to be at the origin of those irregularities. The CFPs deduced before and after the inclusion of spin-orbit coupling, within the L and J ground manifolds, respectively, are shown on Figure S4. They are found to be very similar. It shows that the $J - J$ coupling, which is more important in the beginning of the series, does not affect the CFPs. The model and *ab initio* magnetization matrices (see Table S4) differ more in the first half of the series, especially for Nd and Sm. For the second half of the series, the values of δm are about the same as for the LnZn_{16} series, they decrease and almost vanish for Yb. The largest values of δh are reached for Nd and Sm, meaning that orders higher than 6 are less negligible in those cases. The Slater-Condon parameters which describe the electron-electron interaction increase (see Fig. S3). These tendencies show that the overlap of the metallic and ligand orbitals, which is tiny, decreases in the series. Finally, the difference between AILFT and ITO CFPs should be imputed to electron-electron effects. The former method determines the CFPs at the one-electron level, while the parameters for electron-electron repulsion and spin-orbit coupling are determined independently with additional parameters. In the ITO method, the CFPs are determined from the decomposition of the many-electron wave functions, and describe the other interactions in an effective way. One may not conclude that one approach is more reliable than the other one: AILFT provides one-electron CFPs and, with the knowledge of Slater-Condon parameters and the SO coupling constant, the energy of all the states arising from the $4f^N$ configuration might be calculated. The ITO technique provides effective many electron CFPs, and is specific to each J manifold. For magnetic properties which arise only from the ground J manifold, ITO are recommended since they reproduce exactly the energies of this manifold, while for spectroscopies involving excited J manifolds, AILFT are more suitable.

Paramagnetic NMR shifts

An other domain where CFPs are successfully applied, is the modeling of paramagnetic NMR shifts in lanthanide complexes. Bleaney has shown that the pseudocontact contribution depends on B_0^2 [2]. B_0^2 can be evaluated from pNMR shifts within a lanthanide series, assuming it is constant throughout the series (see Section S4.6 for more details). In ref-

erence [28], the pNMR shifts of the $[\text{Ln}(\text{DPA})_3]^{3-}$ series were measured and modeled using Bleaney’s theory [2] and B_0^2 was found to be 51 with an arbitrary unit applying [54]. It corresponds to 62 cm^{-1} as shown in Section S4.6. This value is four times smaller than the value obtained in this work of 250 cm^{-1} . However, it should be noted that B_0^2 is almost constant in the series, and is the only CFP showing this trend, which supports Bleaney’s theory. It shows that the B_0^2 of Bleaney, which parametrizes the entire magnetic anisotropy in a single is not clearly related to the ‘true’ B_0^2 . It was recently pointed out by Vonci *et al.* [55] that B_0^2 is very sensitive to small structural variations.

Conclusion

CFPs have been extensively used to rationalize the properties of lanthanide complexes. Used as phenomenological parameters, they are fitted on experimental data, which is only possible for high symmetry molecules, as it reduces the number of parameters and avoids the overparametrization in the fitting procedure. With the success of lanthanide complexes as Single Ion Magnets, there is a need to better understand the physics underlying the CFPs, to give guidelines for the synthesis of new molecules, optimizing their desired properties. The model of Rinehart and Long based on electrostatic interaction within an axial symmetry has provided successful guiding lines. In paramagnetic NMR (pNMR), Bleaney’s theory provides a useful background that allows to unravel contact and dipolar contributions to the pNMR shifts, and consequently, to evaluate covalent contributions. This theory is based on CF theory, which reduces to only one CFPs for the whole lanthanide series. The aim of this work was to get more physical insights on the CFPs, by evaluating them from first principles in two series.

Ab initio calculations have already been applied successfully for the determination of Model Hamiltonian parameters. First principles approaches enable a full description of the complexity of molecular systems. *Ab initio* calculations have shown their potential for the determination of model Hamiltonians parameters. This allows to figure out the underlying mechanisms and to estimate the loss of information by projecting the whole complexity on few parameters. The magnetic coupling constant of the Heisenberg Hamiltonian has been extensively described by both wave function based and DFT methods [56]. More recently, *ab initio* calculations were applied for the calculation of anisotropic magnetic couplings [57, 20], and to the ZFS in transition metal complexes [23, 21].

In this work, to determine the CFPs from *ab initio* calculations, two recent methods were applied

on two lanthanide complexes series. The first series is very close to \mathcal{D}_{4d} symmetry and shows a compressed environment due to the presence of metallocrowns. The second series displays an approximate three-fold symmetry due to the presence of counter ions and an oblate environment. The description of those molecular systems by *ab initio* methods allows a description beyond the electrostatic interactions and the determination of the 27 CFPs.

It is the first time that ITO and AILFT methods are compared. AILFT is based on the fitting of the CF matrix written at the orbital level while the ITO method makes a decomposition of the Hamiltonian matrix for a J manifold. These methods lead to very similar CFPs which confirm that the ZFS occurs mostly at the orbital level as was shown previously for lanthanides [31] and for a complex of Ni(II) [37]. However, small discrepancies between AILFT and ITO reveal many-electron effects on the CFPs: they tend to decrease the CFPs in the first half of the series and to increase them in the second half. When calculating CFPs with one or the other method, one should be aware that they do not include the same ingredients. The ITO CFPs are effective and reproduce the energies and composition of a given J manifold and are suitable for spectroscopies probing only one J manifold, like usually magnetic properties. The AILFT CFPs may describe different J manifolds, once the spin-orbit coupling and Slater-Condon parameters are known, and is consequently suitable for spectroscopies involving different J manifolds, like absorption or emission spectroscopies. Trends were discussed by introducing strength parameters, which are rotational invariant. They are shown to be a very convenient tool for the comparison between series by reducing the discussion to only one parameter. Strength parameters were introduced for each order and for each index. The latter are not rotation invariant, but they allow for the quantification of the rotational symmetry, as for the second series, the three fold symmetry.

B_0^2 has opposite signs in the two series in accordance with the respective prolate and oblate environments. Since the CFPs are transferable within a series, magnetic properties follow the sign of the prefactor α_J^2 . Since the LnZn_{16} series is axial, B_0^2 is negative, and the magnetization is axial (planar) for Er (Dy). In the second series, since B_0^2 is positive, the opposite trend is expected. Yet, since the symmetry is not strictly axial, it is not the case: While the Dy complex exhibits an axial magnetization along the pseudo threefold axis (as expected), the Tb derivative exhibits an axial magnetization as well, in a direction perpendicular to that of the Dy complex.

The value of B_0^2 deduced from our calculations is larger than the one deduced from pNMR shifts

in the $[\text{Ln}(\text{DPA})_3]^{3-}$ series using Bleaney’s theory. This reveals that the B_0^2 of Bleaney’s theory is an effective parameter which incorporate other effects. This should be further investigated.

Finally, as expected, the CFPs are transferable along the two series in accordance with Eq. 4, where the reduced parameters α_j^k is related to the metal ion and the B_q^k to the ligands. But they show a systematic decrease in the series, which was already observed in other series. It is shown that within a PC model reproducing the electrostatic potential of the ligands, the CFPs are rather constant in the series; it is shown to be a compensation between the shrinking of the coordination sphere and the greater compactness of the $4f$ orbitals. The decrease of the CFPs in the series is consequently imputed to covalent effects, defined as all effects beyond electrostatic interactions. They comprise bonding, charge transfer and polarization effects. They are not restricted to the overlap between the $4f$ and the ligands’ orbitals. Covalent bonding mostly occurs through the more outer shells orbitals $6s$ and $5d$ orbitals; the change in the electron density of the lanthanide center affects the spitting of the $4f$ orbitals, and thus the CFPs.

Computational details

For all the investigated systems, calculations were performed on the crystallographic structures using SO-CASSCF (Spin-Orbit-Complete Active Space Self Consistent Field) calculations. MOLCAS calculations were performed with the MOLCAS version 7.8 suite of programs [58]. Firstly, a SF-CASSCF (Spin-Free CASSCF) calculation is performed [59] with an active space composed of the seven $4f$ orbitals of the lanthanide ion, and associated electrons, i.e. CAS(n,7). Spin-Orbit (SO) coupling is included by a state interaction with the RASSI (Restricted Active Space State Interaction) method [60]. All the spin states with the highest value of S and 27 singlets (Pr, Tm), 43 doublets (Nd, Er), 86 quartets (Sm), 42 quintets (Eu, Tb), 108 quartets (Dy), 99 triplets (Ho), 35 quartets (Er) or 2 triplets (Tm) were considered for the state interaction. Scalar relativistic effects were taken into account by means of the Douglas-Kroll-Hess transformation [61], and SO integrals are calculated using the AMFI (Atomic Mean-Field Integrals) approximation [62]. For the LnZn_{16} series, Ln and coordinating NO is described by a TZP ANO-RCC basis, atoms of the first cycle of the 12-MC-4 sandwiches with DZP basis and the most remote atoms with SZ. The 24-MC-8 is described by point charges and Zn by ECPs with $1s1p$ [63]. For TbZn_{16} , DyZn_{16} , and ErZn_{16} , $\text{LnZn}_{16}(\text{picHA})_{16}$ structures were considered [25]. For HoZn_{16} , calculations were performed on both the structures of the neighboring ions Dy and Er derivatives, and averaged afterwards. For YbZn_{16} , the $\text{YbZn}_{16}(\text{pizHA})_{16}$ complex was considered [26]. For the $[\text{Ln}(\text{DPA})_3]^{3-}$ series, Ln and O, N, C, H atoms are described with ANO-RCC basis sets of QZP and TZP quality, respectively. g factors were calculated accord-

ing to reference [64] and the CFPs were calculated with a local program written in Mathematica.

All the ORCA-SO-CASSCF calculations were performed using the ORCA 4.0 quantum chemistry package [65]. For the CASSCF calculation, the default CI setting (i.e. CSFCI) was used in combination with the SuperCI and then NR settings for the orbital step. Scalar relativistic effects were accounted for using the second-order scalar relativistic Douglas Kroll Hess (DKH2) Hamiltonian formalism [66, 67]. SO coupling was then accounted for in a mean-field fashion (SOMF) using quasi-degenerate perturbation theory (QDPT) [68], and allowing all CASSCF (SO-free) states from all spin multiplicities to mix through the SOMF operator. To facilitate this task, the CASSCF (SO-free) states were determined using a state-average approach, with all CASSCF states equally weighted.

The all electron scalar relativistic SARC2-QZVP basis sets [69] were used for the lanthanide atoms, and the DEF2-QZVPP basis set [70, 71] for the other atoms (i.e. H, C, N and O). The present DEF2-TZVPP basis sets are an adapted version of the DEF2 basis set from the Karlsruhe group (i.e. Ahlrichs basis set) which is provided in the Turbomole basis set library. They retain the original DEF2 exponents but with contraction coefficients suitable for the DKH scalar relativistic Hamiltonian. Finally, the AUTOAUX feature [72] was used to automatically generate auxiliary basis sets for the resolution of identity approximation (RI-JK) [73], which helps speed up the calculation.

Acknowledgments

This work was supported by the ANR under convention N°ANR-17-CE06-0010. This work was sponsored by the US DOE through the LANL. LANL is operated by Triad National Security, LLC, for the NNSA of US DOE (Contract No. 89233218NCA000001). J.J. thanks LANL for funding through the Director’s Postdoctoral fellowship. This work was supported by the National Science Foundation under grant CHE-1361799 to VLP.

References

- [1] Sessoli, R.; Powell, A. K. Strategies towards single molecule magnets based on lanthanide ions. *Coord. Chem. Rev.* **2009**, *253*, 2328 – 2341.
- [2] Bleaney, B. Nuclear magnetic resonance shifts in solution due to lanthanide ions. *J. Magn. Reson.* **1972**, *8*, 91.
- [3] Bethe, H. Termauspaltung in Kristallen. *Ann. Physik* **1929**, *3*, 133.
- [4] Van Vleck, J. H. Valence strength and the magnetism of complex salts. *J. Chem. Phys.* **1935**, *3*, 807.
- [5] Racah, G. Theory of complex spectra. IV. *Phys. Rev.* **1949**, *76*, 1652.

- [6] Stevens, K. W. H. Matrix elements and operator equivalents connected with the magnetic properties of rare earth ions. *Proc. phys. Soc. A* **1952**, *65*, 209.
- [7] Wybourne, B. G. *Spectroscopic Properties of Rare Earths*; Wiley-Interscience: New-York, 1965.
- [8] Schilder, H.; Lueken, H. Computerized magnetic studies on d, f, d-d, f-f, and d-S, f-S systems under varying ligand and magnetic fields. *J. Magn. Magn. Mater.* **2004**, *281*, 17–26.
- [9] Chilton, N. F.; Anderson, R. P.; Turner, L. D.; Soncini, A.; Murray, K. S. PHI: a powerful new program for the analysis of anisotropic monomeric and exchange-coupled polynuclear d- and f-block complexes. *J. Comput. Chem.* **2013**, *34*, 1164–1175.
- [10] Rinehart, J. D.; Long, J. R. Exploiting single-ion anisotropy in the design of f-element single-molecule magnets. *Chem. Sci.* **2011**, 2078–2085.
- [11] Baldovì, J. J.; Borràs-Almenar, J. J.; Clemente-Juan, J. M.; Coronado, E.; Gaita-Ariño, A. Modeling the properties of lanthanide single-ion magnets using an effective point-charge approach. *Dalton Trans.* **2012**, *41*, 13705.
- [12] Baldovì, J. J.; Clemente-Juan, J. M.; Coronado, E.; Gaita-Ariño, A. Molecular anisotropy analysis of single-ion magnets using an effective electrostatic model. *Inorg. Chem.* **2014**, *53*, 11323–11327.
- [13] Huang, G.; Fernandez-Garcia, G.; Badiane, I.; Camarra, M.; Freslon, S.; Guillou, O.; Daiguebonne, C.; Totti, F.; Cador, O.; Guizouarn, T.; Le Guennic, B.; Bernot, K. Magnetic slow relaxation in a metal-organic framework made of chains of ferromagnetically coupled single-molecule magnets. *Chem. Eur. J.* **2018**, *24*, 6983–6991.
- [14] Chilton, N. F.; Collison, D.; McInnes, E. J. L.; Winpenny, R. E. P.; Soncini, A. An electrostatic model for the determination of magnetic anisotropy in dysprosium complexes. *Nat. Commun.* **2013**, *4*, 2551.
- [15] Choppin, G. R. Structure and thermodynamics of lanthanide and actinide complexes in solution. *Pure Appl. Chem.* **2002**, *27*, 23–42.
- [16] Choppin, G. R. Covalency in f-element bonds. *J. Alloys Compd.* **2002**, *344*, 55–59.
- [17] Neidig, M. L.; Clark, D. L.; Martin, R. L. Covalency in f-element complexes. *Coord. Chem. Rev.* **2013**, *257*, 394 – 406.
- [18] Gupta T., R. G. Singh M.K. Role of Ab Initio calculations in the design and development of lanthanide based single molecule magnets. In *Topics in Organometallic Chemistry*; Springer: Berlin, Heidelberg, 2018.
- [19] Ungur, L. Introduction to the electronic structure, luminescence, and magnetism of lanthanides. In *Lanthanide-Based Multifunctional Materials*; Martín-Ramos, P.; Ramos Silva, M., Eds.; Advanced Nanomaterials Elsevier: , 2018.
- [20] Gendron, F.; Autschbach, J.; Malrieu, J.; Bolvin, H. Magnetic Coupling in the Ce(III) Dimer Ce₂(COT)₃. *Inorg. Chem.* **2019**, *58*, 581–593.
- [21] Chibotaru, L.; Ungur, L. Ab initio calculation of anisotropic magnetic properties of complexes. I. Unique definition of pseudospin Hamiltonians and their derivation. *J. Chem. Phys.* **2012**, *137*, 064112.
- [22] Bolvin, H.; Autschbach, J. Handbook of relativistic quantum chemistry. In ; Liu, W., Ed.; Springer: Berlin, 2017; Chapter Relativistic methods for calculating Electron Paramagnetic Resonance (EPR) parameters.
- [23] Maurice, R.; Bastardis, R.; de Graaf, C.; Suaud, N.; Mallah, T.; Guihéry, N. Universal approach to extract anisotropic spin hamiltonians. *J. Chem. Theory Comput.* **2009**, *5*, 2977.
- [24] Notter, F. P.; Bolvin, H. Optical and magnetic properties of the 5f¹ AnX₆^{q-} series: a theoretical study. *J. Chem. Phys.* **2009**, *130*, 184310.
- [25] Jankolovits, J.; Andolina, C. M.; Kampf, J. W.; Raymond, K. N.; Pecoraro, V. L. Assembly of near-infrared luminescent lanthanide host(host-guest) complexes with a metallacrown sandwich motif. *Angew. Chem. Int. Ed.* **2011**, *50*, 9660–9664.
- [26] Martinić, I.; Eliseeva, S. V.; Nguyen, T. N.; Pecoraro, V. L.; Petoud, S. Near-infrared optical imaging of necrotic cells by photostable lanthanide-based metallacrowns. *J. Am. Chem. Soc.* **2017**, *139*, 8388–8391.
- [27] Kampf, J. W.; Mallah, T.; Pecoraro, V. L. private communication,.
- [28] Autillo, M.; Guerin, L.; Dumas, T.; Grigoriev, M. S.; Fedoseev, A. M.; Cammeli, S.; Solari, P. L.; Guilbaud, P.; Moisy, P.; Bolvin, H.; Berthon, C. Insight of the metal-ligand interaction in f elements complexes by paramagnetic NMR spectroscopy. *Chem. Eur. J.* **2019**, *25*, 4435.
- [29] Atanasov, M.; Aravena, D.; Suturina, E.; Bill, E.; Maganas, D.; Neese, F. First principles approach to the electronic structure, magnetic anisotropy and spin relaxation in mononuclear 3d-transition metal single molecule magnets. *Coord. Chem. Rev.* **2015**, *289*, 177.
- [30] Ungur, L.; Chibotaru, L. F. Ab Initio crystal field for lanthanides. *Chem. Eur. J.* **2017**, *23*, 3708–3718.
- [31] Alessandri, R.; Zulfikri, H.; Autschbach, J.; Bolvin, H. Crystal field in rare-earth complexes: from electrostatics to bonding. *Chem. Eur. J.* **2018**, *24*, 5538–5550.
- [32] Abragam, A.; Bleaney, B. *Electronic paramagnetic resonance of transition ions*; Clarendon Press: Oxford, 1970.
- [33] Görller-Walrand, C.; Binnemans, K. Chapter 155 Rationalization of crystal-field parametrization. In *Handbook on the Physics and Chemistry of Rare Earths*, Vol. 23; Elsevier: , 1996.
- [34] Rudowicz, C.; Qin, J. Noether's theorem and conserved quantities for the crystal- and ligand-field Hamiltonians invariant under continuous rotational symmetry. *Phys. Rev. B* **2003**, *67*, 174420.

- [35] Chang, N. C.; Gruber, J. B.; Leavitt, R. P.; Morrison, C. A. Optical spectra, energy levels, and crystal-field analysis of tripositive rare earth ions in Y₂O₃. I. Kramers ions in C₂ sites. *J. Chem. Phys.* **1982**, *76*, 3877–3889.
- [36] Yeung, Y. Y. Invariants and moments. In *Crystal field handbook*; Newman, D. J.; Ng, B. K. C., Eds.; Cambridge University Press: , 2000.
- [37] Charron, G.; Malkin, E.; Rogez, G.; Batchelor, L. J.; Mazerat, S.; Guillot, R.; Guihéry, N.; Barra, A. L.; Mallah, T.; ; Bolvin, H. Unraveling sigma and pi effects on magnetic anisotropy in cis-NiA₄B₂ complexes: magnetization, HF-HFEPR studies, first-principles calculations, and orbital modeling. *Chem. Eur. J.* **2016**, *22*, 16850–16860.
- [38] Chibotaru, L.; Ceulemans, A.; Bolvin, H. The unique definition of the g tensor of a Kramers doublet. *Phys. Rev. Lett.* **2008**, *101*, 033003.
- [39] Páez Hernández, D.; Bolvin, H. Magnetic properties of a fourfold degenerate state: Np⁴⁺ ion diluted in Cs₂ZrCl₆ crystal. *J. Electron. Spectrosc. Relat. Phenom.* **2014**, *194*, 74.
- [40] Lea, K.; Leask, M.; Wolf, W. The raising of angular momentum degeneracy of f-electron terms by cubic crystal fields. *J. Phys. Chem. Solids* **1962**, *23*, 1381.
- [41] Atanasov, M.; Daul, C. A.; Rauzy, C. A DFT based ligand field theory. In *Optical Spectra and Chemical Bonding in Inorganic Compounds: Special Volume dedicated to Professor Jørgensen I*; Mingos, D. M. P.; Schönherr, T., Eds.; Springer Berlin Heidelberg: Berlin, Heidelberg, 2004.
- [42] Atanasov, M.; Zadrozny, J. M.; Long, J. R.; Neese, F. A theoretical analysis of chemical bonding, vibronic coupling, and magnetic anisotropy in linear iron(II) complexes with single-molecule magnet behavior. *Chem. Sci.* **2013**, *4*, 139–156.
- [43] Aravena, D.; Atanasov, M.; Neese, F. Periodic trends in lanthanide compounds through the eyes of multireference ab initio theory. *Inorg. Chem.* **2016**, *55*, 4457–4469.
- [44] Jung, J.; Atanasov, M.; Neese, F. Ab Initio ligand-field theory analysis and covalency trends in actinide and lanthanide free ions and octahedral complexes. *Inorg. Chem.* **2017**, *56*, 8802–8816.
- [45] Griffith, J. S. *The theory of transition metal ions*; Cambridge University Press: Cambridge, 1961.
- [46] Zare, R. N. *Angular momentum*; Wiley: New-York, 1988.
- [47] Van den Heuvel, W.; Soncini, A. NMR chemical shift as analytical derivative of the Helmholtz free energy. *J. Chem. Phys.* **2013**, *138*, 054113.
- [48] Chow, C. Y.; Bolvin, H.; Campbell, V. E.; Guillot, J. W. R. Kampf; Wernsdorfer, W.; Gendron, F.; Autschbach, J.; Pecoraro, V.; Mallah, T. Assessing the exchange coupling in binuclear lanthanide (III) complexes and the slow relaxation of the magnetization in the antiferromagnetically coupled Dy-2 derivative. *Chem. Sci.* **2015**, *6*, 4148.
- [49] Zhang, P.; Jung, J.; Zhang, L.; Tang, J.; Le Guennic, B. Elucidating the magnetic anisotropy and relaxation dynamics of low-coordinate lanthanide compounds. *Inorg. Chem.* **2016**, *55*, 1905–1911.
- [50] Gagliardi, L.; Lindh, R.; Karlström, G. Local properties of quantum chemical systems: The LoProp approach.. *J. Chem. Phys.* **2004**, *121*, 4494–4500.
- [51] Duan, C.-K.; Tanner, P. A. What use are crystal field parameters? A chemist’s viewpoint. *J. Phys. Chem. A* **2010**, *114*, 6055–6062.
- [52] Faulkner, T. R.; Morley, J. P.; Richardson, F. S.; Schwartz, R. W. The lanthanide crystal field in cubic Cs₂NaLnCl₆ elpasolites. *Mol. Phys.* **1980**, *40*, 1481–1488.
- [53] Ishikawa, N.; Sugita, M.; Okubo, T.; Tanaka, N.; Iino, T.; Kaizu, Y. Determination of ligand-field parameters and f-electronic structures of double-decker bis(phthalocyaninato)lanthanide complexes. *Inorg. Chem.* **2003**, *42*, 2440–2446.
- [54] Reilly, C. N.; Good, B. W.; Desreux, J. F. Structure-independent method for dissecting contact and dipolar NMR shifts in lanthanide complexes and its use in structure determination. *Anal. Chem.* **1975**, *47*, 2110–2116.
- [55] Vonci, M.; Mason, K.; Suturina, E. A.; Frawley, A. T.; Worswick, S. G.; Kuprov, I.; Parker, D.; McInnes, E. J. L.; Chilton, N. F. Rationalization of anomalous pseudocontact shifts and their solvent dependence in a series of C₃-symmetric lanthanide complexes. *J. Am. Chem. Soc.* **2017**, *139*, 14166–14172.
- [56] de Loth, P.; Cassoux, P.; Daudey, J. P.; Malrieu, J. P. Ab initio direct calculation of the singlet-triplet separation in cupric acetate hydrate dimer. *J. Am. Chem. Soc.* **1981**, *103*, 4007.
- [57] Ruamps, R.; Maurice, R.; de Graaf, C.; Guihéry, N. Interplay between local anisotropies in binuclear complexes. *Inorg. Chem.* **2014**, *53*, 4508–4516.
- [58] Aquilante, F.; De Vico, L.; Ferré, N.; Ghigo, G.; Malmqvist, P.-A.; Neogrády, P.; Pedersen, T. B.; Pitonak, M.; Reiher, M.; Roos, B.; Serrano-Andrés, M.; Urban, M.; Veryazov, V.; Lindh, R. MOLCAS 7: The next generation. *J. Comput. Chem.* **2010**, *31*, 224.
- [59] Roos, B. O.; Taylor, P. R.; Siegbahn, P. E. M. A complete active space SCF method (CASSCF) using a density matrix formulated super-CI approach. *Chem. Phys.* **1980**, *48*, 157.
- [60] Malmqvist, P.-A.; Roos, B. O.; Schimmelpfennig, B. The restricted active space (RAS) state interaction approach with spin-orbit coupling. *Chem. Phys. Lett.* **2002**, *357*, 230.
- [61] Hess, B. A. Relativistic electronic-structure calculations employing a two-component no-pair formalism with external-field projection operators. *Phys. Rev. A* **1986**, *33*, 3742.
- [62] Hess, B. A.; Marian, C. M.; Wahlgren, U.; Gropen, O. A mean-field spin-orbit method applicable to correlated wavefunctions. *Chem. Phys. Lett.* **1996**, *251*, 365.

- [63] López-Moraza, S.; Pascual, J. L.; Barandiarán, Z. Ab initio model potential embedded-cluster study of V^{2+} -doped fluoroperovskites: Effects of different hosts on the local distortion and electronic structure of ${}^4T_{2g}$ - ${}^4A_{2g}$ laser levels. *The Journal of Chemical Physics* **1995**, *103*, 2117–2125.
- [64] Bolvin, H. An alternative approach to the g-matrix: theory and applications. *ChemPhysChem* **2006**, *7*, 1575.
- [65] Neese, F. Software update: the ORCA program system, version 4.0. *Wiley Interdisciplinary Reviews: Computational Molecular Science* **8**, e1327.
- [66] Reiher, M. Douglas-Kroll-Hess theory: a relativistic electrons-only theory for chemistry. *Theor. Chem. Acc.* **2006**, *116*, 241–252.
- [67] Nakajima, T.; Hirao, K. The Douglas-Kroll-Hess approach. *Chem. Rev.* **2012**, *112*, 385–402.
- [68] Neese, F. Efficient and accurate approximations to the molecular spin-orbit coupling operator and their use in molecular g-tensor calculations. *J. Chem. Phys.* **2005**, *122*, 034107.
- [69] Aravena, D.; Neese, F.; Pantazis, D. A. Improved segmented all-electron relativistically contracted basis sets for the lanthanides. *J. Chem. Theory Comput.* **2016**, *12*, 1148–1156.
- [70] Weigend, F.; Furche, F.; Ahlrichs, R. Gaussian basis sets of quadruple zeta valence quality for atoms H–Kr. *J. Chem. Phys.* **2003**, *119*, 12753–12762.
- [71] Weigend, F.; Ahlrichs, R. Balanced basis sets of split valence triple zeta valence and quadruple zeta valence quality for H to Rn: Design and assessment of accuracy. *Phys. Chem. Chem. Phys.* **2005**, *7*, 3297–3305.
- [72] Stoychev, G. L.; Auer, A. A.; Neese, F. Automatic generation of auxiliary basis sets. *Journal of Chemical Theory and Computation* **2017**, *13*, 554–562.
- [73] Neese, F. An improvement of the resolution of the identity approximation for the formation of the Coulomb matrix. *J. Chem. Theory Comput.* **2003**, *24*, 1740–1747.